

An Experimental Analysis of Hot Aisle Containment Systems

Sadegh Khalili¹, Husam Alissa², Anuroop Desu³, Bahgat Sammakia¹, Kanad Ghose³
¹ Department of Mechanical Engineering, Binghamton University-SUNY, NY 13905, USA
² Microsoft, WA 98052, USA
³ Department of Computer Science, Binghamton University-SUNY, NY 13905, USA
Email: skhalil6@binghamton.edu

ABSTRACT

In recent years, various airflow containment systems have been deployed in data centers to improve the cooling efficiency by minimizing the mixing of hot and cold air streams. The goal of this study is the experimental investigation of passive and active hot aisle containment (HAC) systems. Also investigated, will be the dynamic interaction between HAC and information technology equipment (ITE). In addition, various provisioning levels of HAC are studied. In this study, a chimney exhaust rack (CER) is considered as the HAC system. The rack is populated by 22 commercial 2-RU servers and one network switch. Four scenarios with and without the presence of cold and hot aisle containments are investigated and compared. The transient pressure build-up inside the rack, servers' fan speed, inlet air temperatures (IAT), IT power consumption, and CPU temperatures are monitored and operating data recorded. In addition, IAT of selected servers is measured using external temperature sensors and compared with data available via the Intelligent Platform Management Interface (IPMI). To the best of authors' knowledge, this is the first experimental study in which a HAC system is analyzed using commercial ITE in a white space. It is observed that presence of backpressure can lead to a false high IPMI IAT reading. Consequently, a cascade rise in servers' fan speed is observed, which increases the backpressure and worsen the situation. As a result, the thermal performance of ITE and power consumption of the rack are affected. Furthermore, it is shown that the backpressure can affect the accuracy of common data center efficiency metrics.

KEYWORDS: Experimental Study, Containment, HAC, Chimney, Active, Passive, White Space.

NOMENCLATURE

AFC	active flow curve
aHAC	active hot aisle containment
CA	cold aisle
CAC	cold aisle containment
CER	chimney exhaust rack
CPU	central processing unit
CRAH	computer room air handler
DCiE	data center infrastructure efficiency
HA	hot aisle
HAC	hot aisle containment
IAT	inlet air temperature
IT	information technology
ITE	information technology equipment
IPMI	intelligent platform management interface
MLC	mechanical load component
P	pressure, in. wc (Pa)
pHAC	passive hot aisle containment

PUE	power usage effectiveness
RU	rack unit
t	time, s
UPS	uninterruptible power supply

Subscripts

a	ambient
---	---------

INTRODUCTION

According to 2016 United States data center energy usage report [1], data centers in the U.S. consumed approximately 70 billion kWh (1.8% of total electricity consumption in the U.S.) in 2014. This report forecasts the data centers energy consumption will increase by 4% from 2014-2020 and reach 73 billion kWh in 2020. This is a significant shift from the 90% percent increase that was estimated for 2000-2005 and the 24% percent increase that was estimated for 2005-2010. The report suggests that the rate of increase in data centers energy consumption can be decreased through energy-efficiency improvements, consolidation of data center compute activity from smaller data centers to larger data centers, adoption of data center energy efficiency improvement technologies, and improved data center operations management. The deployment of air containment systems is an important energy saving strategy for cooling optimization of data centers. Equally important, the accelerated use of data centers, increase of IT rack power density, as well as the need for maintaining reliable operation temperature, has urged engineers to develop improved thermal solutions for various applications within data centers. Currently, there are two main types of containment systems, namely hot and cold aisle containment. In both hot and cold aisle containment systems an alignment of IT-rack rows in a consistent hot aisle / cold aisle (HA/CA) alignment is required. In a cold aisle containment (CAC) system the supply of cold air is enclosed and the hot air exhaust from IT devices is returned to the cooling units through the uncontained room space resulting in an elevated room temperature. Therefore, special care should be given to non-racked ITE and other devices such as electric outlets, lighting, fire suppression systems, etc. The advantages and disadvantages of CAC have been discussed in numerous studies. In a case study by Muralidharan et al. [2], a 22% saving in cooling energy is achieved by installing a CAC system over a standard HA/CA arrangement. Nemati et al. [3] compared the performance of row-based cooling in open and CAC configurations. Shrivastava and Ibrahim [4], as well as Alissa et al. [5], compared the thermal performance of HA/CA and CAC systems during cooling failures. Alissa et al. [5] observed that the available uptime is longer in a CAC system compared to an HA/CA system when data from external inlet air temperature sensors are considered while opposite behavior is seen when IPMI data is taken into account. In other words, Alissa et al. [5]

discovered that the external temperature fields may not reflect the ITE thermal performance during airflow mismatches due to a cooling failure in a CAC system. It should be noted that although deploying a CAC system decreases the mixing of hot and cold air streams and prevents hot air recirculation, it also minimizes the overall volume of available cold air to ITE in case of a loss of cooling.

A HAC system encloses the hot air stream from the time it is exhausted by ITE until it is returned to the cooling units and provides a cooler environment in the data center room as a whole. Generally, CAC and HAC systems have different characteristics such as distinct leakage paths. In addition, a HAC system contains the hot air from ITE's exhaust to cooling units and therefore, the rest of the data center space becomes a large cold-air supply room with a temperature close to the supply air temperature. This provides a large volume of available cooling air to the ITE which can extend the ride through time in case of cooling mismatches. A cooling mismatch may occur in various scenarios such as cooling equipment failure (chilled water, chiller, pump, and/or blower failures). In addition, virtualization and varying IT load can change the airflow demand in different parts of a data center and create local airflow mismatches. A cooling mismatch can endure for minutes depending on the cause and extent of failure as well as response time of control systems and maintenance workers.

In HAC systems, hot air is confined to a hot aisle and therefore does not affect the non-racked equipment and the work environment. Niemann et. al [6] performed a theoretical analysis on the impact of CAC and HAC systems on the efficiency of a data center. In this study, it is shown that HAC presents more opportunities in energy saving compared to CAC as it allows higher supply air temperatures. An elevated supply temperature has multiple benefits such as the more efficient operation of the cooling units and increased economizer mode hours. In addition, an increased supply temperature can help to mitigate humidity problems in humid climates, and reduces costs associated with dehumidifiers. Niemann et al [6] concluded that HAC should be deployed as the default containment solution in all new data center designs. Shrivastava et al. [7] numerically compared the CAC and HAC systems versus a HA/CA configuration. However, the impact of backpressure on ITE airflow is ignored in [7], and it is assumed that CER and HAC are thermally equivalent.

A CER is a hot air containment solution that can be utilized to reduce hot spots in data centers. In a CER system, a chimney exhaust, as well as a solid rear door, is installed on the rack to capture and direct the ITE exhaust air to a drop ceiling return air plenum or into a space high above the rack inlet. Implementing CER systems result in a cooler work environment in the hot aisle compared to typical HAC systems. Furthermore, CERs can be utilized locally to reduce hot spots in a data center. In addition to all the features of CAC and HAC, a fully contained CER (in which both hot and cold aisles are contained) provides an opportunity for isolating high-density racks from the rest of data center. The chimneys deployed on racks are available either fan powered or non-fan powered - active and passive systems, respectively. In a passive CER, server fans and cooling units are responsible for air ventilation.

Despite the advantages of containing hot air, the pressure buildup in the hot aisle may limit the airflow rate through ITE. This problem can be addressed by increasing the suction pressure of the data center room exhaust fan or installing a rack exhaust fan for assisting exhaust airflow. Installing a chimney fan offers multiple benefits such as reduced backpressure, decreased hot air leakage to cold aisle through rack gaps as well as decreased load and power consumption on ITE fans. In addition, larger fans generally operate at higher efficiencies than smaller fans of proportional size [8]. Therefore, installing an active chimney could potentially result in lower fans speed of individual ITE, and consequently lowers total rack power. Furthermore, the chimney fans can assist server fans during airflow imbalances. However, it should be noted that connecting chimney fans to the uninterruptible power supply (UPS) of a data center may limit the UPS power available to ITE. It is worth mentioning that the presence of backpressure is not only limited to HAC, but it also can be found in airflow imbalances in CAC systems, e.g. in case of airside cooling failure, or in an under-provisioned CAC.

To the best of authors' knowledge, there is a lack of experimental data for HAC systems in publication and this is the first experimental study on HAC systems utilizing commercial ITE. Such experimental data is crucial to determine, optimize and maintain optimal and reliable operational conditions in the data centers that utilize hot air containment solutions. In this paper, the impact of containing hot air within a server rack is analyzed experimentally and compared with a CAC system. The transient pressure build-up inside the rack, central processing unit (CPU) temperatures, IAT, servers' fan speed and ITE power consumption are presented for passive and active systems. In the base scenario (scenario 1), a standard HA/CA arrangement and a CAC system are considered and studied. In the CAC system, cold air is supplied to the ITE via a localized CAC in front of the rack while the hot air is released into the room as a large hot aisle. Next, for a comprehensive evaluation of different containment systems, three containment systems are considered, namely, passive HAC (pHAC), active HAC (aHAC) and hybrid containment (HC). In the HAC systems, the hot air is enclosed and extracted from the top near the back of the rack while the room is considered as a large cold aisle. The passive and active HAC systems are studied in the second and third scenarios, respectively. A combination of HAC and CAC systems (hybrid containment) is considered as the last scenario in which both hot and cold aisles are enclosed. In addition, various negative pressures are applied to the rack exhaust vent to simulate an aHAC. The experiments are carried out at the ES2 research data center lab at Binghamton University. The air temperature and pressure at both supply and return sides are measured using external sensors, and reported. Furthermore, the servers' IAT are extracted from IPMI data and compared with data from external sensors. Finally, the accuracy of common data center efficiency metrics when backpressure is present is discussed.

EXPERIMENTAL SETUP AND PROCEDURES

For the present study, a 47-RU rack is populated with 22 Dell PowerEdge 2950 2-RU servers and one Cisco Nexus 2248TP-GE Fabric Extender. The servers are selected from the

same model and generation to limit the number of pertinent parameters in this study. Also, a Dell PowerEdge R730 is tested in the rack to investigate the dependency of results on the ITE. Because of the obstructions, no server could be mounted on the first rack unit at the bottom of the rack. Therefore, a 2-RU blanking panel is installed at the bottom of the rack to blank the empty RU slots. A perforated tile is deployed in front of the rack to supply cooling air at 64° F (18° C) from a raised floor. The tile is 32% open and slightly directional, which redirects the cooling air towards the face of the rack and air intakes of the ITE. The overall outside dimension of the rack is 87.5" H × 28" W × 48" D (222 cm × 71 cm W × 122 cm D). The rack posts are made of hollow profile and have mounting slots. The slots on hollow posts can be a path for cold air bypass or hot air recirculation. Hence, all the slots on the rack's front posts are sealed to achieve a good segregation of hot and cold air. Furthermore, the gaps between the servers' front panel are covered by gap sealing strips. The rack offers the option of hot air enclosure, i.e. the exhaust hot air from servers can be extracted through an 18" (46 cm) diameter round opening at the top near the back of the rack when the removable solid rear door is in place. With the rear door closed, a 15" (38 cm) deep chamber is available between the outlet of the servers and the rack's rear door. The rack's exhaust opening is ducted to the inlet of a wind tunnel (Fig. 1a) to measure the rack's exhaust airflow rate in scenarios 2, 3 and 4. All the duct connections are sealed to eliminate any leakage in the ductwork. Also, a perimeter rubber gasket around the rear door frame properly seals the rear side. The dimensions of the local CAC are 99" H × 32" W × 32" D (251 cm × 81 cm × 81 cm). Figures 1b to 1d shows location of the local CAC, the rack's front face, and location of instrumentations and perforated floor tile. The temperature sensors and pressure probes are outlined in red and blue, respectively.

The servers' power data are collected from a three-phase Server Technology power distribution unit (PDU) through an internal data center network. In the studied cases, the minimum and maximum of total rack power are measured as 8.5 kW and 9.8 kW, respectively. All the servers boot from the network into a Debian Jessie environment. A Linux service is utilized for collecting IPMI data from servers [9]. This service uses Linux coretemp module which provides individual CPU temperatures. In addition, servers' fan speeds and IPMI inlet temperatures are collected through OpenIPMI libraries. This service periodically collects the above-mentioned data and sends it to a centralized application using TCP/IP protocol. The temperature measurements are carried out using Degree-C UAS1200LP airflow and temperature sensors. The resolution of temperature measurements is ±0.18° F (±0.1° C). The temperature sensors are mounted at the inlet of servers 1, 11 and 22 (at the top, middle and bottom of the rack). Additionally, one temperature sensor is attached to the front of the intake duct of the network switch above server 1. The pressure data are collected using Bapi ZPT-LR pressure sensor with measurement range of 1" wc (248.84 Pa) and accuracy of ±0.25% of range. In this study, all the reported pressure measurements are differential pressures with respect to the pressure in the data center room. The location of instrumentations is presented in Fig. 1c and 1d. Two pressure probes are mounted in the cold aisle at top and middle of the

rack's front face. Also, three pressure probes are installed on the rear door of the rack to monitor pressure changes in the hot aisle with time and height of the rack. Three holes are drilled at the base of chimney's duct-work, interconnected, and connected to a pressure sensor by vinyl tubing (Fig. 1e). This provides a pressure measuring point at the base of the chimney.

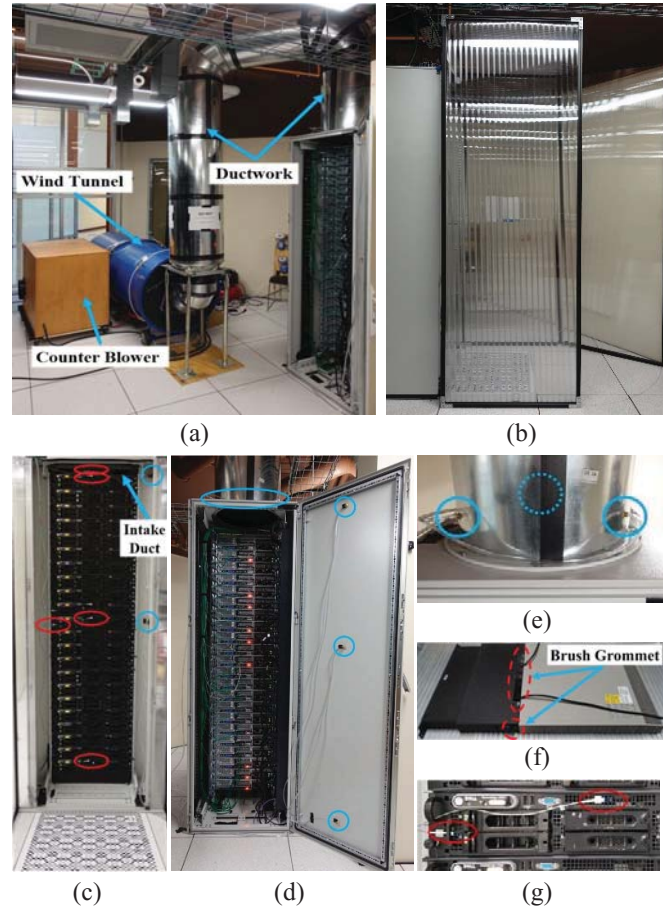


Fig. 1: Experimental setup and instrumentation: a) chimney ductwork, b) local CAC (door is open), c) instrumentations in the cold aisle and location of intake duct and the perforated floor tile, d) instrumentations in the hot aisle, e) location of pressure probes at the base of chimney, f) intake duct (black) for the network switch and location of brush grommet, g) location of temperature sensors in front of server 11.

The network switch is mounted on the back of the server rack, and its intake is ducted to the cold aisle using a commercial intake duct. The intake duct has a brush grommet that provides space for passing power cables of the network switch (Fig. 1f). The round exhaust vent at the top of the rack is ducted to a wind tunnel (Fig. 1a). The wind tunnel (designed in accordance with AMCA 210-99/ASHRAE 51-1999) is used for measuring the chimney airflow rate and establishing various provisioning levels by adjusting static pressures at the chimney base. The flow rate through the chimney is calculated by measuring the pressure drop across a nozzle array in the wind tunnel. Straightening screens are installed upstream and downstream of the nozzle array to break up turbulence in the airstream and provide a uniform flow approaching the nozzle

array. The wind tunnel is attached to a counter blower which can be controlled by a solid-state speed controller. In addition, the flow rate through wind tunnel can be controlled by a sliding gate valve called blast gate.

The free delivery point of a sample server and the network switch are measured experimentally by mounting the ITE on the wind tunnel with a proper nozzle selection and maintaining zero pressure differential across the ITE. Furthermore, the relation between ITE flow rate and the differential pressure across it (active flow curve) is extracted by varying supplied airflow rate and measuring the differential pressure. The active flow curves (AFC) for the server operating at the base and maximum fan speeds, and the network switch are presented in Fig. 2a and 2b, respectively. It is worth mentioning that the fan speed of the network switch did not change in the studied cases. The AFCs for other fan speeds may be derived by utilizing affinity laws [10]. In this paper, the supplied airflow rate through the tile is adjusted to be approximately equal to the sum of ITE airflow demand at the free delivery point at the beginning of all the studied cases. Utilizing the extracted AFCs, when the servers' fans running at base speed (6860 rpm), the required airflow for provisioning the rack is calculated as 980 CFM (0.462 m³/s). The tile airflow rate is measured using a flow hood with back pressure compensation. It should be mentioned that the tile flow rate is set and measured at the beginning of each test but is not regulated during the tests. The plenum depth under the rack is 2 ft (0.61 m) and ceiling height is 17 ft (5.18 m). The details about the layout of ES2 data center lab can be found in [5].

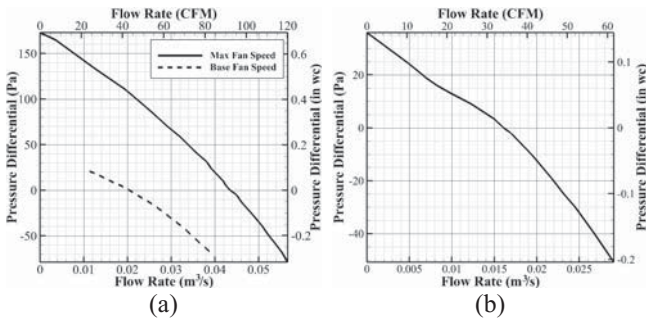


Fig. 2: Active flow curve: a) Dell Power Edge 2950, b) Cisco Nexus 2248TP-GE.

EXPERIMENTAL PROCEDURES

Scenario 1: Baseline Cases

For this study, a standard HA/CA arrangement (case 1-1) and a CAC system (case 1-2) are considered as the baseline cases. In case 1-2, a local CAC is deployed in front of the rack and cold air is supplied to CAC through a perforated floor tile in front of the rack. The rear door of the rack is removed and the servers' exhaust hot air is released into the room in both cases of this scenario. Therefore, no backpressure is imposed on the ITE in this scenario. Also, the impact of CPU utilization on the power consumption of the rack is addressed in this scenario.

Scenario 2: Passive Hot Aisle Containment

In this scenario, after assuring a steady state in the HA/CA arrangement, the rear door of the rack is installed at $t = 0$ to build a HAC system. The servers' exhaust hot air leaves the

HAC through the round vent on the top of the rack (chimney base). Nemati et. al [11] compared steady-state and transient thermal behavior in CAC, HAC and CER systems numerically. Their results showed that pressure at the base of chimney can be negative, zero or positive depending on the distance from cooling units. In this study, the differential pressure between the base of the chimney and room is maintained at 0 Pa. The counter blower speed is adjusted manually to achieve a constant pressure at the base of the chimney as the servers' fans ramp up. The door of the local CAC is left open and ITE is supplied with cold air from both the perforated floor tile and the room. Considering the dimensions of the local CAC, the impact of containment's walls and ceiling on the airflow field is assumed to be insignificant when the CAC door is open.

Scenario 3: Active Hot Aisle Containment

Similar to scenario 2, the room and supplied cold air through the perforated tile are the sources of cooling air in scenario 3. Therefore, the pressure in front of the ITE is the room pressure. Three different HAC provisioning scenarios including under-provisioning, neutrally-provisioning, and over-provisioning, are considered and investigated. In this study, provisioning is defined based on the differential pressure across the ITE. Based on this definition, a neutrally provisioned HAC is a HAC in which the differential pressure across the ITE is zero ($P_{HAC} = P_a$ in this scenario). In other words, the ITE operates at its free delivery point in a neutrally provisioned HAC. Accordingly, under-provisioned and over provisioned HACs are cases in which positive and negative backpressures are imposed on the ITE, respectively. Because the pressure at the top of the hot aisle could be affected by air suction through the chimney, the differential pressure across the middle of the rack is considered as the measure for evaluation of provisioning level in this study. The pressure at the rack outlet is considered as the control parameter and maintained at various values to simulate various operating speeds of a chimney fan.

Scenario 4: Hybrid Containment

In this scenario, an HC system is investigated in which CAC and HAC are simultaneously installed. This is accomplished by closing the door of the local CAC, and installing the rear door on the rack. Similar to scenario 3, under-provisioned, neutrally provisioned and over-provisioned cases are studied.

TEST DATA AND ANALYSIS

In this section, the results of the test scenarios are presented and discussed. The pressure and temperature measurements from both external and IPMI sensors are reported. It is worth repeating that all the reported pressures are differential pressures with respect to the room pressure. The servers are numbered from 1 to 22 from top to bottom of the rack.

Scenario 1: Baseline Cases

This scenario provides reference data for comparison purposes. In the initial step, the rear door of the rack was removed and the door of the local CAC is left open (standard HA/CA arrangement) and the servers were operating in idle mode (no CPU utilization). The tile flow rate is measured three times using a commercial flow hood at the beginning of the experiment. The tile average flow rate is calculated as 1,014 CFM (0.478 m³/s) which is slightly more than the required

airflow for neutrally-provisioning the rack (5% over-provisioning). After assuring a steady state, data is gathered for 600 seconds. Next, at $t = 600$ s, the servers' CPUs are stressed 100% by running the Linux stress test on maximum available cores (case 1-1). Finally, at $t = 4,000$ s, the door of the local CAC is closed (case 1-2). The infrared thermography of the rack's face at the final steady state of the base scenario is available in the appendix. Figures 3-5 present the transient variation of parameters of interest during the described steps. A slight increase in IPMI IAT is seen after stressing the CPUs while the discrete sensors show no change in the IAT of servers. This increase can be due to heat conduction from CPU chips to the IPMI IAT sensor through printed circuit boards (PCBs), hot air recirculation inside the servers, or both. Considering the fact that the IPMI IAT sensor and CPUs are mounted on separate PCBs and are not directly connected, the effect of heat conduction from CPU chips to the IPMI IAT sensor should be insignificant. In addition, the considerable distance between the CPU junctions and the IPMI IAT sensor in front of the server strengthens this hypothesis that conduction plays an insignificant role in this phenomenon.

It is observed that containing the cold aisle slightly decrease the inlet temperature. That is due to the elimination of room air entrainment by containing the cold aisle. An interesting observation is the high IAT at the face of the network switch (Fig. 3), which increases with the servers' outlet temperature shown in Fig. 4. This is while the air temperature at the top of the rack (front of the intake duct) is significantly lower (see Fig. 3). This observation demonstrates a hot air recirculation through the brush grommet (see Fig. 1f) into the intake duct of the network switch.

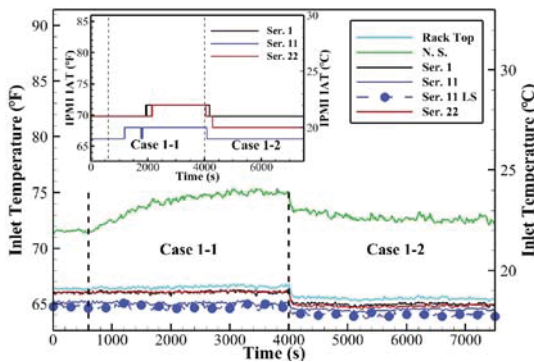


Fig. 3: Discrete and IPMI IAT of the selected ITE - scenario 1

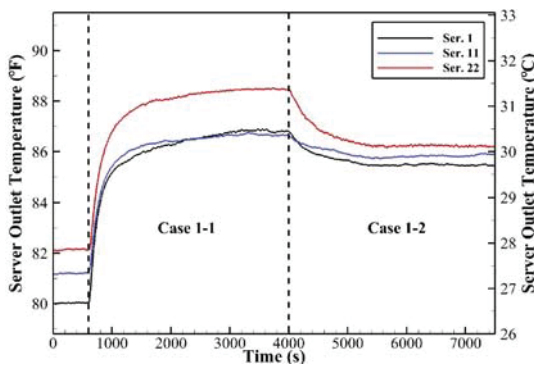


Fig. 4: Servers outlet temperature - scenario 1

Figure 5 shows that, at this IAT, the fan speed of the servers does not change after stressing the CPUs. It is worth mentioning that each server has four hot-pluggable cooling fans that operate at slightly different speeds. In this study, an average of the speed of four fans for the selected servers is calculated and reported at each time step. The increase in power consumption due to CPUs' load is clear in Fig. 5. In addition, the rise in the total rack power is presented in this figure as a percentage of total increase in the rack power with respect to the rack power at the beginning of the test. It is observed that stressing CPUs increased the total rack power by 50%.

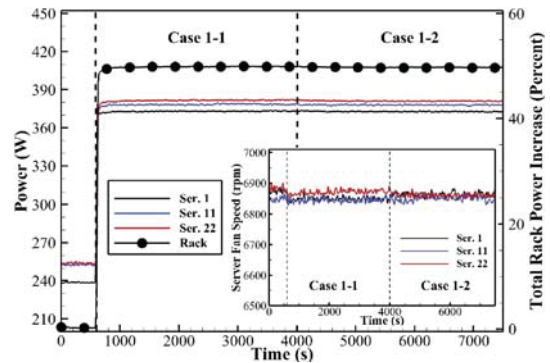


Fig. 5: Power consumption of the servers (left axis), the percentage increment in the rack's total power (right axis) and averaged fan speed of the selected servers - scenario 1

Scenario 2: Passive Hot Aisle Containment

Figures 6 to 10 present the transient data for a pHAC system. The system is let to reach a steady state in a standard HA/CA arrangement before closure of the rear door at $t = 0$. Hence, the room is treated as a large cold aisle, and pressure in front of the ITE was equal to the room pressure. The tile flow rate is measured as 1,009 CFM ($0.476 \text{ m}^3/\text{s}$) at the beginning of this scenario. The pressure at the rack outlet (base of the chimney's ductwork) is controlled at $0 \pm 1 \text{ Pa}$ ($0 \pm 0.004 \text{ in. wc}$) by adjusting the rate of airflow draw through the chimney. Figure 6 shows the pressure variation at different locations on the rack rear door. It is observed that the pressure inside HAC increases with time which indicates an increasing backpressure build-up. This is due to the increase in servers' fan speed and consequently, increased servers' exhaust airflow rate, pressure, and air velocity.

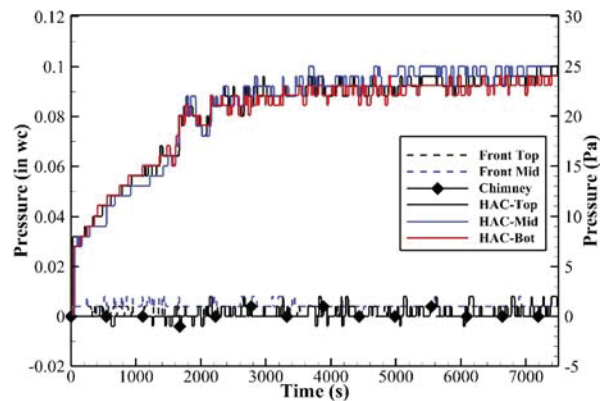


Fig. 6: Pressure variation in the hot and cold aisles - case 2

A higher velocity jet creates higher stagnation pressure on the HAC door where the pressure sensors are mounted. In addition, no significant difference is observed between the pressure measurements at different elevations inside the HAC. The pressure at the bottom of the rack is slightly lower than the rest of the HAC at the end of the test. This lower pressure can be due to the void space available under server 22. This space provides more room for the exhaust air of the servers near the bottom of the rack. In addition, air leakage from the gap around the blanking panel relieves the developed backpressure. Also, this space allows access to an available room between the mounting rail and the side walls of the rack, which is connected to the rack's exhaust and provides a route to the rack's exhaust. The oscillations in the pressure measurements are mainly due to sudden changes in fan speed of the servers and the resolution of the pressure measurements. Furthermore, the speed of the counter blower is adjusted manually based on the pressure readings at the base of the chimney, which cause some small oscillations in pressure readings.

The presence of the backpressure can have consequences. Figure 7 shows an elevated temperature at the inlet of the servers and network switch. Also, it is seen that the IPMI IAT of servers increases with time. It should be mentioned that the supply air temperature of the computer room air handler (CRAH) units was fixed and no change in the room temperature is observed during all the tests of this study. Therefore, the increasing IPMI IAT in Fig. 7 is not due to a change in the cold air temperature. Figure 8 presents an infrared thermography of the rack. The temperature scale is shown on the right side of the thermal images. A hot area on the left side of the servers' face is seen in the thermal image. In addition, hot areas in front of the network switch's intake duct and the blanking panel are observed (at the top and bottom of the rack, respectively). The high surface temperature at the inlet of the intake duct and server 22, as well as the edges of the servers (left edge particularly), is due to the presence of recirculation. A hot air recirculation can mix with cold air and increase the temperature of cooling air at the inlet of the ITE. Figure 7 shows elevated temperatures at the left side of a server 11 (middle of the rack, see Fig. 1g), and in front of the intake duct of the switch (top of the rack). This observation confirms the presence of hot air recirculation. In addition, it is observed that temperature at the inlet of the switch is significantly higher than in case 1 (Fig. 3). This high temperature at the inlet of the network switch shows that presence of backpressure enhances the recirculation through the brush grommet. Furthermore, Figs. 7 and 8 also reveal that the extent of hot air leakage through the brush grommet is not only limited to the network switch, but it also can affect the IAT of the servers in a close proximity of the switch (e.g. server 1). Similarly, hot air leakage from the gaps around the blanking panel caused an increase in IAT of server 22.

The difference between the IPMI IAT and discrete temperatures in Fig. 7 is significantly larger than this difference in the first scenario. This large difference cannot be due to heat conduction as discussed earlier. A potential explanation can be an internal hot air recirculation inside the servers. Further investigations on this matter are out of the scope of this paper and authors plan to study this problem in the future.

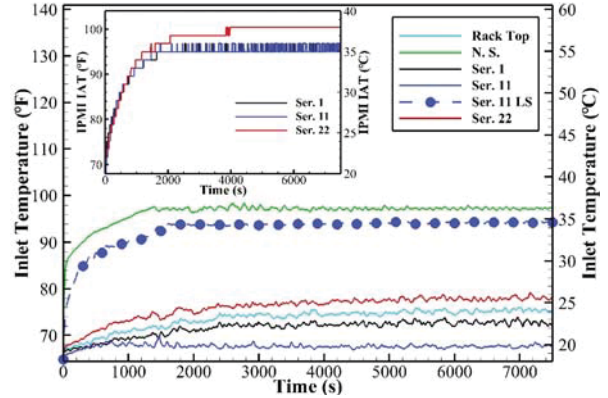


Fig. 7: Discrete and IPMI IAT of the selected ITE - case 2

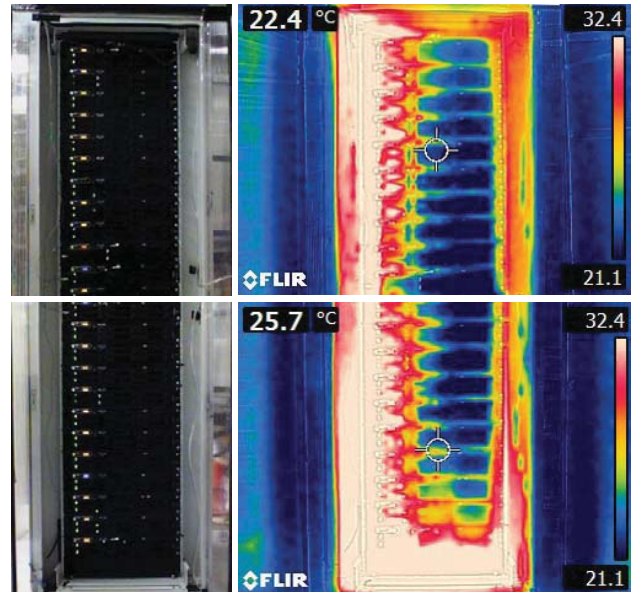


Fig. 8: Thermal image of the top and bottom half of the rack's front face (temperatures in degree C)

Figure 9 shows the fan speed variation of the selected servers during the test period. The fan speed of the servers is adjusted automatically to maintain component temperatures in a safe range. This is done by the servers' fan controller based on various internal sensors' readings. The IPMI IAT and the CPU junction temperatures are important parameters in the fan control strategy of the servers. By comparing Fig. 7 and 9, a similar behavior is seen between IPMI IAT and the fan speed variations. The variation of the CPU junction temperature for selected servers is presented in Fig. 10. The initial temperature rise in Fig.10 is due to the sudden drop in the servers flow rate as a result of the introduced backpressure. Later on, no significant change is seen in the CPU junction temperatures of servers 1 and 11. Therefore, it is perceived that the false high IPMI IAT should play the dominant role in the elevation of fan speed in this experiment. It is worth mentioning that the higher CPU junction temperature of server 22 can be due to the higher IAT for this server (see Fig. 7) that is because of the hot air recirculation from the gap around the blanking panel.

A surge in fan speeds is seen in Fig. 9 after $t = 1,500s$. At this moment, the fans in server 22 ramp up to their maximum

speed as the IPMI IAT touches 96.8°F (36°C). This large step increase in fan speed is observed in the rest of the servers within a few minutes. A large change in fan speed leads to an elevated backpressure inside the HAC ($t \approx 1600\text{s}$ in Fig. 6). This is followed by a large increase (i.e. overshoot) in the counter blower speed to maintain the pressure at the control point (base of the chimney in this study), which drops the pressure inside the HAC ($t \approx 2000\text{s}$ in Fig. 6). As a result, the backpressure drops and consequently the IPMI IAT and fan speed decrease. This process repeated multiple times but the amplitude of the oscillations decreased with time as shown in Fig. 9. These oscillations in a rack level may not cause a problem, however, in a data center scale, this can cause instabilities in the cooling systems, damage the equipment and waste energy. The oscillations can be minimized by having a more continuous change in fan speed of the servers instead of large step changes.

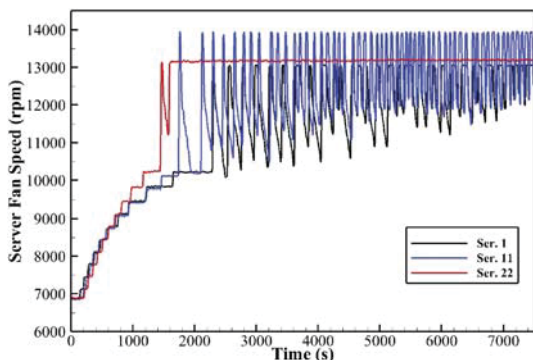


Fig. 9: Averaged fan speed of the selected servers - case 2

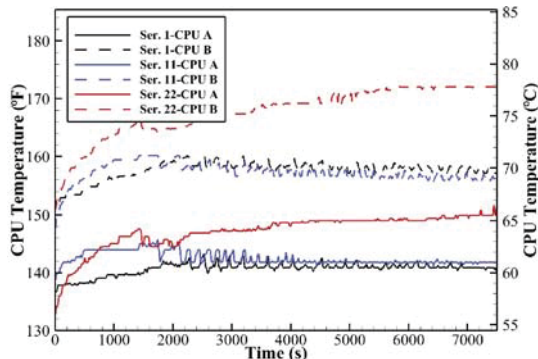


Fig. 10: CPU junction temperatures of the selected servers - case 2

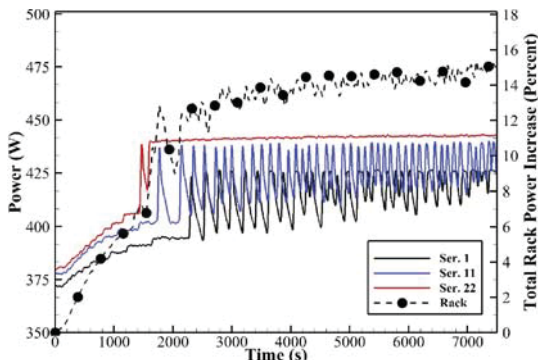


Fig. 11: Power consumption of the servers and the percentage increment in the rack's total power - case 2

The power consumption of the selected servers and the increment in total rack power is shown in Fig. 11. It is seen that the total rack power increased by about 15% at the end of the experiment which is significant. The increase in power consumption is primarily due to the increase in the servers' fan speed as the CPU utilization of the servers is fixed at 100%. It should be noted that at lower CPU utilizations, the ratio of the power consumed by the server fans to the total power consumption of the server is higher (due to lower CPU power consumption). Therefore, in lower CPU utilizations, the percentage of total rack power increase due to fan speed rise is predicted to be higher (up to 25% for the current setup).

Scenario 3: Active Hot Aisle Containment

In this scenario, the pressure at the base of the chimney is considered as the control parameter during the experiment, i.e. pressure at this point is maintained at certain values of interest. For the neutral-provisioning case (case 3-1), the pressure at the outlet of the rack (chimney base) is maintained at $-0.092 \pm .004$ in. wc (-23 ± 1 Pa) to achieve equal pressures in the middle of the cold aisle and the middle of the rack's rear door (zero backpressure). For the under-provisioning case (case 3-2), the counter blower speed is decreased to reduce the rate of air draw through the chimney and let a pressure buildup inside the HAC. In this case, the pressure at the base of the chimney is controlled at $-0.040 \pm .004$ in. wc (-10 ± 1 Pa). For over-provisioning case (case 3-3), the rate of air extraction is increased to maintain the pressure at the base of the chimney at $-0.145 \pm .004$ in. wc (-36 ± 1 Pa). In all cases of this scenario, no significant variation in the pressure across the HAC height is seen (less than 1 Pa difference).

- Case 3-1: Neutrally-Provisioned HAC

Figure 12 shows an approximately zero backpressure which remains constant during the test period. As it was mentioned earlier, the installed tile is slightly directional and redirects air toward the face of the rack. As a result, air impinges to the rack face and creates slightly higher pressure and small oscillations in the pressure in the cold aisle. This observation is explained and discussed in [12].

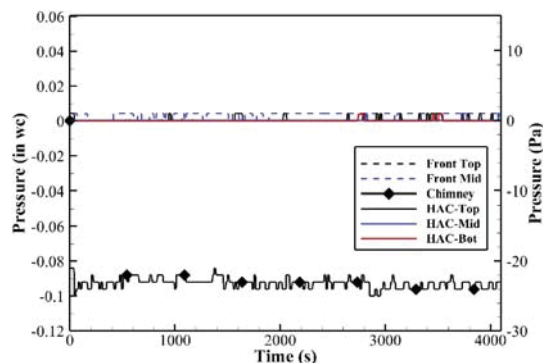


Fig. 12: Pressure variation in the hot and cold aisles - case 3-1

Figure 13 demonstrates that the discrete and IPMI temperature sensors show constant values. In addition, the difference between the internal (IPMI) and external temperature measurements is decreased in this case compared to case 2. Figure 14 shows no considerable change in the fan speed of the

servers and the overall power consumption of the rack during the test. The flow rate through the chimney is approximately constant in case 3-1 and is measured as 1023 ± 5 CFM (0.483 ± 0.002 m³/s).

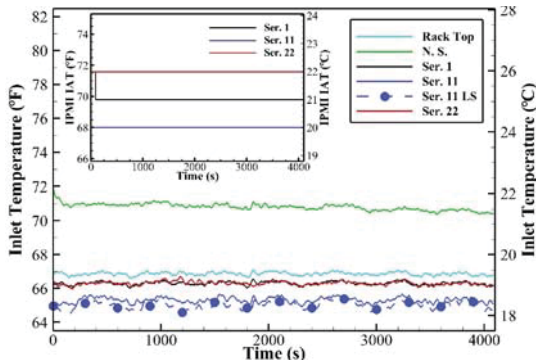


Fig. 13: Discrete and IPMI IAT of the selected ITE - case 3-1

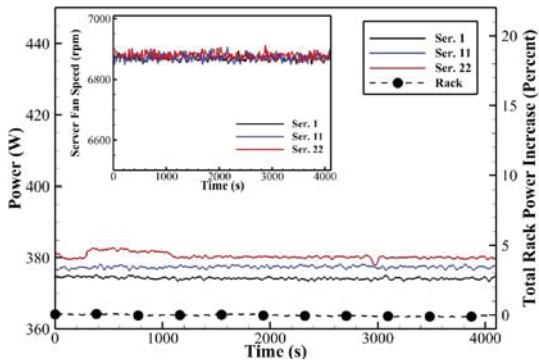


Fig. 14: IT power consumption, the percentage increment in the rack power and averaged fan speed - case 3-1

- Case 3-2: Under-Provisioned HAC

Figure 15 presents the variation of pressure at different locations with time. As the pressure at the base of the chimney is higher than the neutrally provisioned HAC (case 3-1), a backpressure buildup is observed in this case. This backpressure increased with time until the system reached a steady state. In the steady state, the continuous increase in the IPMI IAT and consequently, the increase in the servers' fan speed and power consumption stopped (Figs. 16 and 17). The results showed higher IPMI IAT, fan speed and power consumption for server 22. This shows that ITE close to blanking panels are more prone to the consequences of a recirculation.

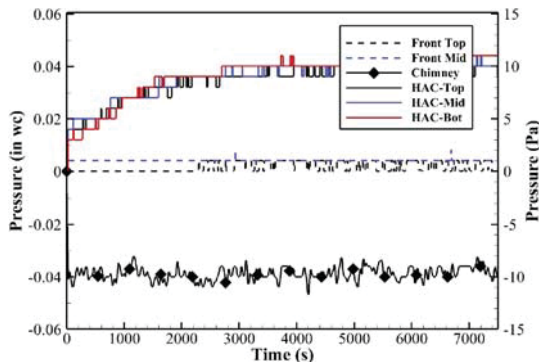


Fig. 15: Pressure variation in the hot and cold aisles - case 3-2

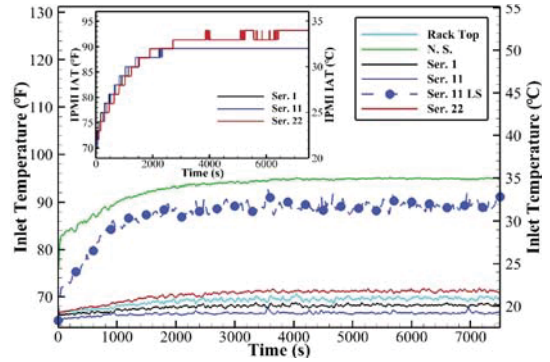


Fig. 16: Discrete and IPMI IAT of the selected ITE - case 3-2

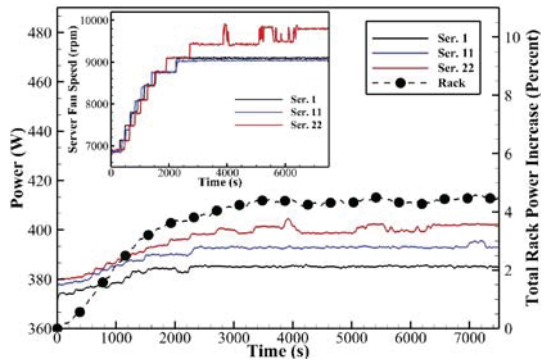


Fig. 17: IT power consumption, the percentage increment in the rack power and averaged fan speed - case 3-2

- Case 3-3: Over-Provisioned HAC

The variation of pressure with time at different locations in the cold and hot aisles is represented in Fig. 18. In this case, the rate of air draw through the chimney is higher than the neutrally provisioned HAC (case 3-1). A negative backpressure is observed inside the HAC which assists the server fans.

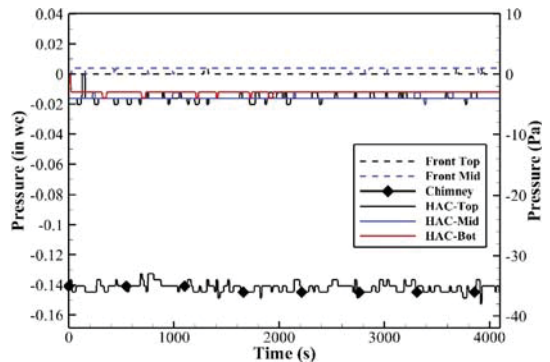


Fig. 18: Pressure variation in the hot and cold aisles - case 3-3

Figure 19 shows a slight decrease in IPMI IAT of the servers. Also, it is seen that the IAT of the switch approached the temperature in front of the intake duct (top of the rack). This shows that a negative backpressure limits the recirculation through the brush grommet that connects the switch to the intake duct. Furthermore, a minimal difference is seen between the internal (IPMI) and external temperature readings in this case. The decrease in the IPMI IAT of the servers in presence of a negative backpressure along with the results of the prior cases is evidence for a server-level phenomenon as a result of

backpressure which affects IPMI IAT readings and consequently, the server's fan speed and power consumption. As it was mentioned earlier, authors plan to investigate the cause of dependency of IPMI IAT measurements on backpressure in a server-level study in the future.

According to the experimental data, it is seen that the IPMI IAT threshold corresponding to the initial fan ramp up is 78.8°F (26°C) for the tested servers. Therefore, the servers' fans operate at their base speed when IPMI IAT is lower than this threshold. Hence, no change in the fan speed and the power consumption of the servers is observed in Fig. 20. The flow rate through the chimney for case 3-3 is measured as 1176 ± 10 CFM (0.555 ± 0.005 m³/s).

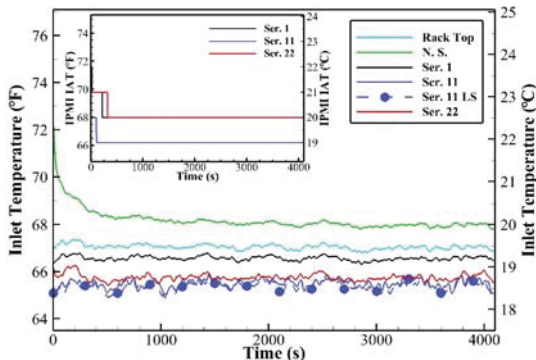


Fig. 19: Discrete and IPMI IAT of the selected ITE - case 3-3

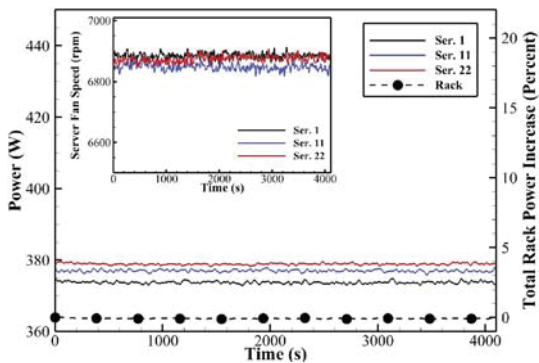


Fig. 20: IT power consumption, the percentage increment in the rack power and averaged fan speed - case 3-3

Scenario 4: Hybrid Containment

Similar to scenario 3, various provisioning levels in the HAC are achieved by regulating the speed of the counter blower. In this scenario, the system was in a standard HA/CA arrangement before hot and cold aisles are contained at $t=0$. For neutrally-provisioning case (zero pressure differential across server 11), the pressure at the base of the chimney is controlled at $-0.092 \pm .004$ in. wc (-23 ± 1 Pa). For the under- and over-provisioning cases (case 4-2 and 4-3), the pressure at the base of the chimney is controlled at $-0.040 \pm .004$ in. wc (-10 ± 1 Pa) and $-0.145 \pm .004$ in. wc (-36 ± 1 Pa), respectively. The perforated floor tile is the only source of the cold air in this scenario. It should be mentioned that the flow rate of the tile is measured at the beginning of each test. The tile flow rate is not regulated during the tests of this scenario. However, the area of the raised floor is 215 m² (2315 ft²) which offers a large plenum compared to the volume of the local CAC and therefore, the

variations in the plenum pressure due to changes in the CAC pressure is expected to be small.

- Case 4-1: Neutrally-Provisioned Hybrid Containment

The tile flow rate is measured as 975 CFM (0.460 m³/s). The free delivery points of the servers and network switch are extracted from the AFCs (Figs. 2a and 2b) and are used to calculate the theoretical required airflow rate for neutrally provisioning the rack. The calculations showed 971 CFM (0.458 m³/s) is needed to provision the ITE (with servers' fans running at base speed), which is close to the measured tile airflow rate (less than 1% error).

The variation of pressure at different locations in the cold and hot aisles is shown in Fig. 21. It is seen that the pressure in the middle of hot and cold aisles are equally higher than the room pressure ($+0.004$ in. wc or 1 Pa). This demonstrates that the free delivery point of ITE can be utilized for finding required airflow rate for neutrally provisioning a chimney cabinet when the hot and cold zones are segregated properly. The positive pressure inside the CAC is due to the directionality of the installed tile as well as the slightly higher supply airflow rate than the required flow rate for neutrally provisioning the ITE. Figure 22 shows a small initial drop in the IAT of the servers (for $t < 250$ s) which is due to the elimination of air entrainment from the room by containing the cold aisle. The fan speed and power consumption of the servers show no considerable change during the test period (Fig. 23). It should be noted that the pressure at the base of the chimney is significantly lower than P_{HAC} . The magnitude of the difference depends on the airflow rate of ITE, geometry of the chimney and HAC as well as the quality of segregation between cold and hot aisle.

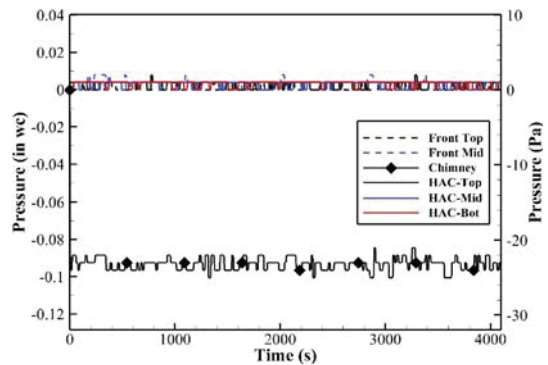


Fig. 21: Pressure variation in the hot and cold aisles - case 4-1

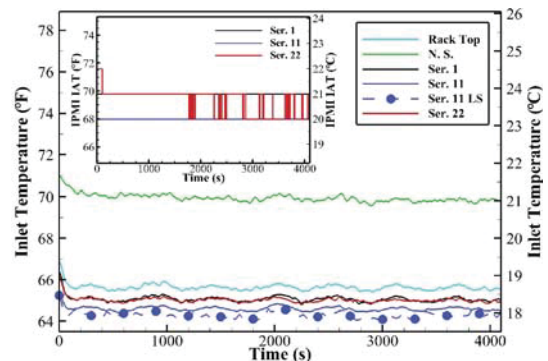


Fig. 22: Discrete and IPMI IAT of the selected ITE - case 4-1

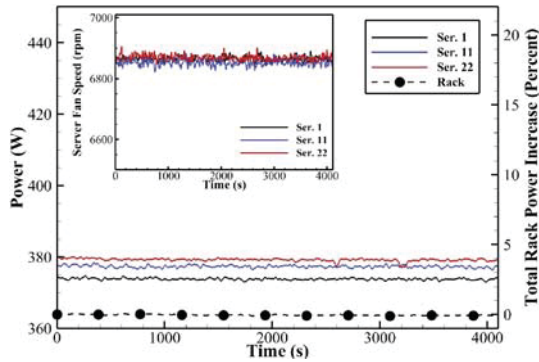


Fig. 23: IT power consumption, the percentage increment in the rack power and averaged fan speed - case 4-1

- Case 4-2: Under-Provisioned Hybrid Containment

In this case, the tile flow rate is measured as 905 CFM ($0.427 \text{ m}^3/\text{s}$) at the beginning of the test. An important observation in Fig. 24 is a positive pressure inside the CAC while the ITE is under-provisioned ($P_{\text{HAC}} > P_{\text{CAC}}$). The developed backpressure in the HAC causes hot air leakage from HAC (with higher pressure) to CAC (with lower pressure). Besides, as it is discussed before, the presence of back pressure decreases the airflow rate through the ITE. Therefore, the available airflow rate inside the CAC (the summation of supplied cold airflow rate through the perforated tile and the hot air leakage into CAC) is higher than the airflow through ITE. This excess airflow rate cannot escape to the room since the cold aisle is contained. Consequently, a positive pressure inside the CAC is developed. A quick comparison between Figs. 15 and 24 reveals that although the magnitude of pressures is higher in case 4-2, the back pressure ($P_{\text{HAC}} - P_{\text{CAC}}$) is lower in case 4-2 compared to case 3-2 (under-provisioned HAC). This is while the pressure at the base of the chimney is controlled at $-0.040 \pm .004 \text{ in. wc}$ ($-10 \pm 1 \text{ Pa}$) in the both cases. This lower difference can be explained by the pressure buildup inside the CAC which decreases the imposed backpressure on ITE.

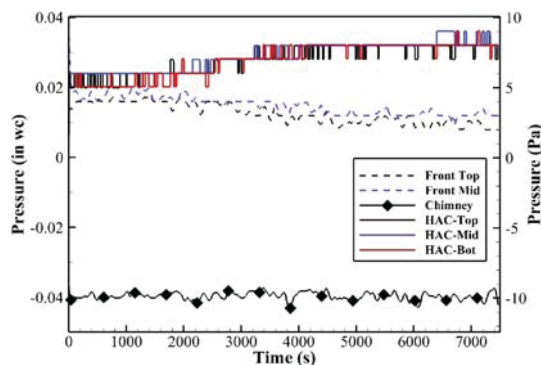


Fig. 24: Pressure variation in the hot and cold aisles - case 4-2

The temperature of CPU junctions of server 11 in cases 3-2 and 4-2 are compared in Fig. 25. It is seen that the junction temperatures in case 4-2 are lower than corresponding temperatures in case 3-2. The lower temperature of CPUs in server 11 is an evidence of higher airflow rate through the server due to the lower imposed backpressure on the ITE. It should be mentioned that discrete sensors show similar IAT for server 11 in cases 3-2 and 4-2 (see Figs. 17 and 26).

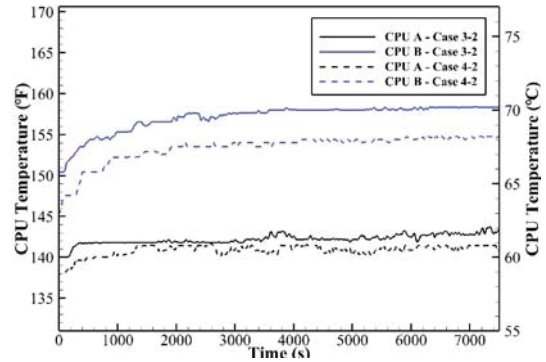


Fig. 25: Comparison of CPU junction temperature between case 3-2 and case 4-2.

The industry has always been monitoring the provisioning level by measuring differential pressure between inside either the hot or cold containment and room. A significant finding of this test is that the differential pressure between CAC and room is not a good measure for determining the provisioning level in an HC system, e.g. CER. In addition, it is observed that the difference between pressures at the base of chimney duct and the HAC can be significant. Therefore, the pressure inside chimney also should not be considered for determining the provisioning level. The authors suggest that the differential pressure across the ITE should be measured and considered as the determinative parameter for evaluation of the provisioning level of ITE.

The variation of the IPMI and discrete inlet temperatures over time is presented in Fig. 26. The IPMI temperature sensors show lower temperatures compared to case 3-2. Similar behavior is seen in the discrete temperature measurements at the top and bottom of the rack. This slight difference has two causes. First, the room air entrainment is eliminated by containing the cold aisle. Second, less hot air leaks from the hot aisle to the cold aisle through the intake duct and gaps around the blanking panel due to the lower backpressure in this case. Therefore, HC systems feature a lower rate of hot and cold air mix. However, the pressures in CAC and HAC are related in a HC system which creates a more complex behavior. In addition, slightly lower temperatures are observed at the intake of the network switch in this case compared to case 3-2. Figure 27 shows that the servers' fan speed and the increment in the total rack power increase with time. However, the increases are smaller in case 4-2.

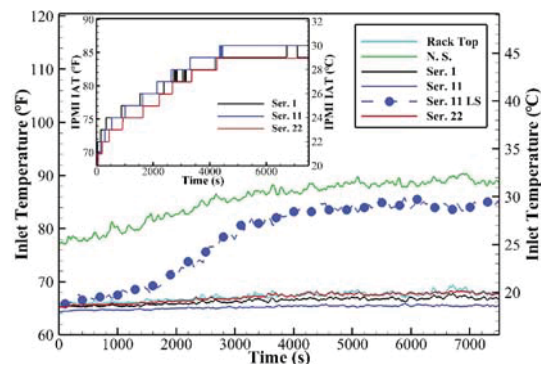


Fig. 26: Discrete and IPMI IAT of the selected ITE - case 4-2

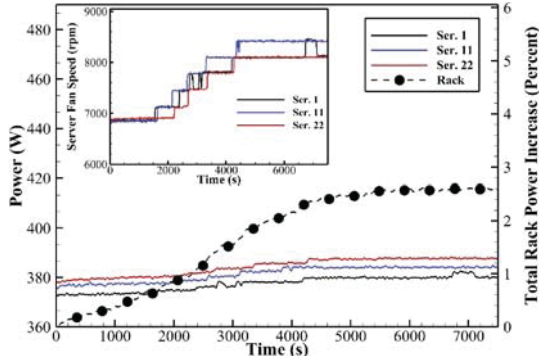


Fig. 27: IT power consumption, the percentage increment in the rack power and averaged fan speed - case 4-2

- Case 4-3: Over- Provisioned Hybrid Containment

The results for the over-provisioned HC are represented in Figs. 28 to 30. A slight negative pressure is observed inside the CAC in Fig. 28 which is because of the over-provisioning of the HAC. The airflow rate through the tile was measured at 1,010 CFM (slightly more than required airflow for provisioning the ITE) before enclosing the hot and cold aisles. After enclosing both the hot and cold aisles, the tile flow rate increased to 1,065 CFM due to the negative pressure inside the CAC. Figure 29 shows a small drop in IPMI IAT of the servers while the discrete sensors show no change in the IAT of the servers. Again, this is an evidence for the impact of the pressure field on IPMI sensor readings. In addition, the IAT of the network switch decreased in an over-provisioned HC system. This shows that the over-provisioning the HAC can help with reducing the hot air recirculation. Figure 30 shows no considerable change in the servers' fan speed and power during the test.

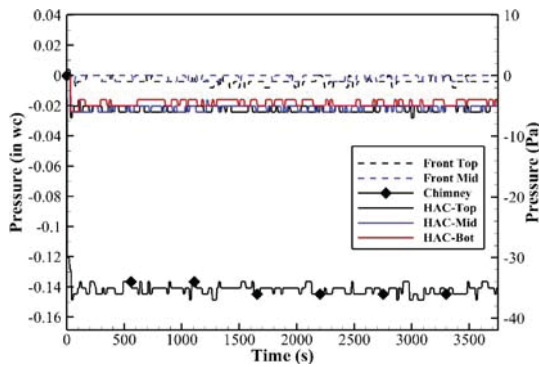


Fig. 28: Pressure variation in the hot and cold aisles - case 4-3

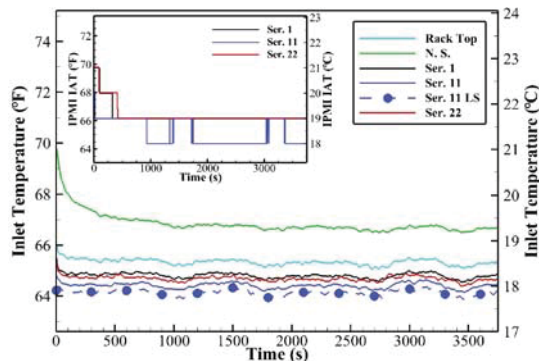


Fig. 29: Discrete and IPMI IAT of the selected ITE - case 4-3

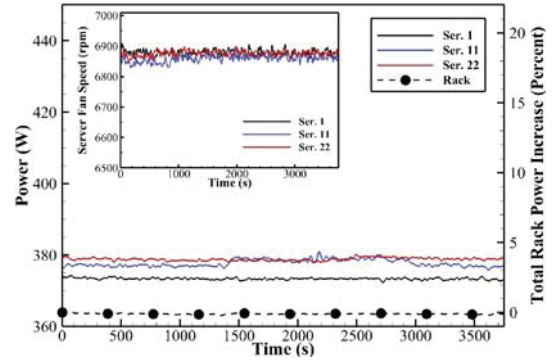


Fig. 30: IT power consumption, the percentage increment in the rack power and averaged fan speed - case 4-3

Table 1 compares the processors' temperature and averaged fans speed of server 11 at the end of the studied cases. The highest fan speed is observed in the pHAC scenario. In addition, lower fan speed and CPU temperatures are achieved in the HC compared to the aHAC system. A consistent observation in all the cases is the higher temperature of CPU-B compared to CPU-A that can be due to an internal recirculation.

Table 1: Fan speed and CPU temperatures of Ser. 11 at the end of each case

Scen. #	Case #	Fan Speed (rpm)	CPU-A	CPU-B
1	1-1	6860	138 °F (59 °C)	145 °F (63 °C)
	1-2	6860	137 °F (58.5 °C)	143 °F (61.5 °C)
2	-	13970	142 °F (61 °C)	156 °F (69 °C)
	3-1	6860	138 °F (59 °C)	147 °F (64 °C)
3	3-2	9060	144 °F (62 °C)	158 °F (70 °C)
	3-3	6860	137 °F (58.5 °C)	145 °F (63 °C)
4	4-1	6860	137 °F (58.5 °C)	145 °F (63 °C)
	4-2	8400	141 °F (60.5 °C)	154 °F (68 °C)
	4-3	6860	136 °F (58 °C)	144 °F (62 °C)

Test with a Newer Generation Server

The purpose of this section is to investigate the dependency of results on ITE. In this part, server 10 is replaced with a newer generation server (Dell PowerEdge R730) server and the test procedure of scenario 2 (pHAC) is repeated. This server utilizes 6 fans (compared to 4 fans in Dell PowerEdge 2950) that allows operation in a lower fan speed. The results showed a similar behavior in the new generation server including false high IPMI IAT and elevated fan speed (Fig. 31). However, a larger surge increase in fan speed of the R730 is observed.

It should be noted that in this test one new generation server was placed in the middle of the rack and between Dell PowerEdge 2950 servers. Therefore, the thermal performance of the other servers in a close proximity to the R730 could have an impact on the behavior of the new generation server. Finally, it should be mentioned that the findings of this study are based on the results for the described experimental setup and test procedures. Further investigations with different HAC dimensions, chimney geometry, and type of ITE are required to achieve a better understanding of the impact of various parameters on the pressure buildup inside HAC systems.

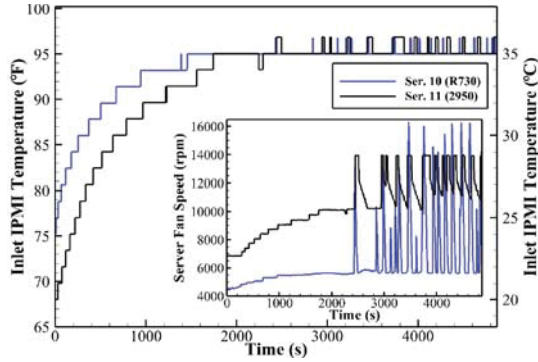


Fig. 31: IPMI IAT and averaged fan speed of the selected servers – pHAC

A Comment on Data Center Efficiency Metrics

The power usage effectiveness (PUE) and Data center infrastructure efficiency (DCiE) are popular tools for evaluating data centers [13]. The PUE of a data center can be calculated using Eq. (1).

$$PUE = \frac{1}{DCiE} = \frac{\text{Total Facility power}}{\text{ITE Power}} \quad (1)$$

where ITE power is the energy delivered to ITE. The ITE power includes the power used by CPU, GPU, RAM, fans, power supplies, etc. In an aHAC system, the power consumption of chimney fan is considered as a part of the energy required for cooling systems. On the other hand, energy used by a server's fan is considered as a part of ITE power and is added to both the nominator and denominator in Eq. (1). This can lead to misleading PUE calculations. For example, two data centers DC 1 and DC 2 with identical facility power consumption can be considered in which servers of type 1 and type 2 are deployed, respectively. Assume that the servers types 1 and 2 have identical power consumptions but operate with different servers' fan speed resulting from variations in fan control strategies, installed components, environmental conditions such as backpressure, etc. According to Eq. (1), the PUE of the above-mentioned data centers is identical. However, the productive work (useful compute work) in DC 1 and DC 2 is different. A similar scenario can be present in comparison of various containment systems, e.g. CAC versus HAC when fans of ITE operate at different speeds. Therefore, the presence of backpressure can also affect the accuracy of common data center efficiency metrics. Hence, PUE (and DCiE) may not be accurate and descriptive tools for comparison of various containment systems in their current forms. Recently, ASHRAE introduced mechanical load component (MLC) as an improved measure for the efficiency of the mechanical side in data centers. The MLC is defined as the sum of all cooling, fan, pump, and heat rejection power divided by the data center ITE power. Because ITE fan power is included as a part of cooling power, MLC can provide a better measure for evaluation of the cooling efficiency and comparison of various containment systems in data centers.

Conclusions

This paper, for the first time in literature, presents an experimental investigation on the active and passive HAC systems. A 47 RU rack is populated with 22 commercial 2-RU

servers and one network switch. The maximum power load of the rack reached 9.8 kW in this study. The hot aisle is enclosed by deploying a rear door and hot air is exhausted through an 18" diameter round chimney. The thermal performance of the ITE, rack power and backpressure buildup in passive, active, and HC systems is investigated under various provisioning levels. The IAT of the servers is measured and reported using the discrete sensors. In addition, the transient impact of backpressure on the IPMI IAT, CPU junction temperature, servers' fan speed and rack power load is presented. It is observed that backpressure buildup in pHAC and under-provisioned aHAC systems can have a significant impact on the power consumption and potentially the reliability of ITE. In the presence of backpressure, a significant discrepancy in IAT measurements of IPMI and discrete sensors is seen, which increased with backpressure. In other words, IPMI IAT sensor showed false high IAT readings when a backpressure had been imposed on the servers. This false IPMI IAT caused an elevated servers' fan speed which increased the backpressure further. Consequently, a cascade increase in fan speed of the servers is observed which worsened the situation. Besides increasing the total power consumption in a data center, an elevated fan speed can lower lifetime of fans and decrease the reliability of the equipment. Furthermore, it is shown that backpressure limits the airflow rate through the ITE. On the other hand, it is observed that a negative backpressure decreases the difference between the readings of IPMI and external sensors. The dependency of IPMI IAT on the backpressure reveals a server level phenomenon that can be investigated in a separate study.

This study shows that the discrete temperature fields do not accurately reflect the thermal performance of the ITE, particularly in the presence of backpressure. In addition, it is seen that a surge increase in the servers' fan speed can lead to a sudden change in the backpressure and consequently, instability in the cooling system. Furthermore, the widely used data center efficiency metric, PUE, is not enough descriptive in presence of backpressure.

In summary, the presence of backpressure can lead to an increased fan speed and power consumption of the ITE. A maximum of 15% increase in total rack power due to the false high IPMI readings is seen in this study. This increase is predicted to rise to 25% for servers with no-compute load (idling mode) for the current experimental setup. In addition, it is suggested that differential pressure between hot and cold zones should be considered as the determinative parameter for evaluation of the provisioning level. Furthermore, it is observed that installing chimney fan can significantly improve the thermal performance in pHAC systems when backpressure is present. The bottom line of this study is that the backpressure can affect the thermal performance of ITE, decrease the overall efficiency and reliability of data centers, and should be avoided.

Acknowledgment

The authors would like to thank D. Mendo from Comcast and K. D. Hall from the Binghamton University computer science department. We would also like to thank the ES2 partner universities for their support and advice. This work is supported by NSF IUCRC Award No. IIP-1738793 and MRI Award No. CNS1040666.

References

- [1] A. Shehabi, S. Smith, D. Sartor, R. Brown, M. Herrlin, J. Koomey, E. Masanet, and W. Lintner, "United States Data Center Energy Usage Report," 2016.
- [2] M. Bharath, S. K. Shrivastava, M. Ibrahim, S. A. Alkharabsheh, and B. G. Sammakia, "Impact of Cold Aisle Containment on Thermal Performance of Data Center," in *InterPACK2013-73201*, 2013, no. 55768, pp. 1–5.
- [3] K. Nemati, H. Alissa, and B. Sammakia, "Performance of Temperature Controlled Perimeter and Row-Based Cooling Systems in Open and Containment Environment," in *ASME International Mechanical Engineering Congress and Exposition*, 2015, no. 57502, p. V08BT10A047.
- [4] S. K. Shrivastava and M. Ibrahim, "Benefit of Cold Aisle Containment During Cooling Failure," *ASME 2013 Int. Tech. Conf. Exhib. Packag. Integr. Electron. Photonic Microsystems*, no. 55768, p. V002T09A021, 2013.
- [5] H. A. Alissa, K. Nemati, B. G. Sammakia, M. J. Seymour, D. Tipton, R. Mendo, D. W. Demetriou, K. Schneebeili, R. Tipton, D. Mendo, D. W. Demetriou, and K. Schneebeili, "Chip to Chiller Experimental Cooling Failure Analysis of Data Centers: The Interaction Between IT and Facility," *IEEE Trans. Components, Packag. Manuf. Technol.*, vol. 6, no. 9, pp. 1361–1378, 2016.
- [6] J. Niemann, K. Brown, and V. Avelar, "Impact of hot and cold aisle containment on data center temperature and efficiency," *Schneider Electr. Data Cent. Sci. Center, White Pap.*, vol. 135, pp. 1–14, 2011.
- [7] S. K. Shrivastava, A. R. Calder, M. Ibrahim, and T. Park, "Quantitative comparison of air containment systems," *Intersoc. Conf. Therm. Thermomechanical Phenom. Electron. Syst. ITherm*, pp. 68–77, 2012.
- [8] R. Eiland, J. E. Fernandes, B. Nagendran, V. Mulay, and D. Agonafer, "Effectiveness of Rack-Level Fans—Part I: Energy Savings Through Consolidation," *J. Electron. Packag.*, vol. 139, no. 4, p. 41011, 2017.
- [9] T. J. Stachecki and K. Ghose, "Short-term Load Prediction and Energy-Aware Load Balancing for Data Centers Serving Online Requests*," 2015.
- [10] H. A. Alissa, K. Nemati, B. G. Sammakia, K. Schneebeili, R. Schmidt, and M. J. Seymour, "Chip to Facility Ramifications of Containment Solution on IT Airflow and Uptime," *IEEE Trans. Components, Packag. Manuf. Technol.*, vol. 6, no. 1, pp. 67–78, 2016.
- [11] K. Nemati, H. A. Alissa, B. T. Murray, and B. Sammakia, "Steady-state and transient comparison of cold and hot aisle containment and chimney," in *In Thermal and Thermomechanical Phenomena in Electronic Systems (ITherm), 15th IEEE Intersociety Conference on*, 2016, pp. 1435–1443.
- [12] S. Khalili, M. Tradat, K. Nemati, M. Seymour, and B. Sammakia, "Impact of Tile Design on the Thermal Performance of Open and Enclosed Aisles," *J. Electron. Packag.*, vol. 140(1), pp. 10907-10907–12, 2018.
- [13] C. Belady, A. Rawson, J. Pflueger, and T. Cader, "Green grid data center power efficiency metrics: PUE and DCIE," Technical report, Green Grid, 2008.

Appendix

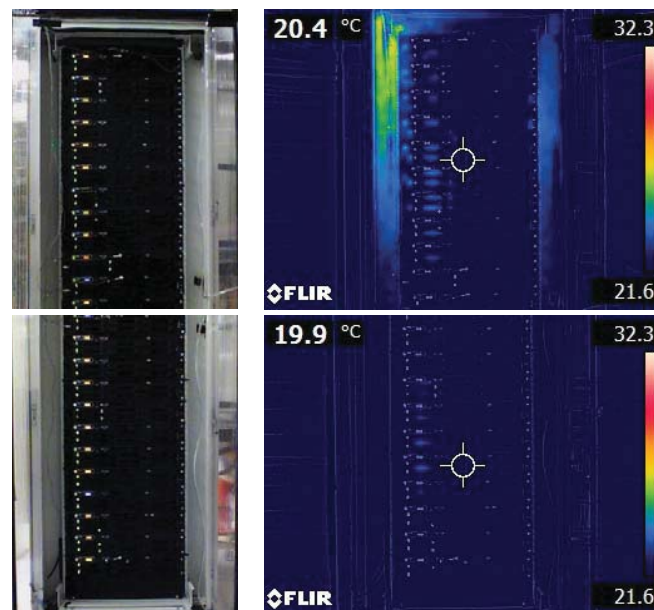


Fig. 1A: Thermal image of the top and bottom half of the rack's front face (temperatures in degree C) – Scenario 1